Available online at www.joac.info

ISSN: 2278-1862

Journal of Applicable Chemistry

2017, 6 (1): 176-189

(International Peer Reviewed Journal)

Corrosion Inhibition of Cu in Nitric Acid Solution using Asafoetida Extract (ASFE) as Green Inhibitor

A.S. Fouda[1], S.M. Rashwan[2], H. E. Ibrahim[2] and F. Salamony[1]

1. Department of Chemistry, Faculty of Science, El-Mansoura University, El-Mansoura-35516, **EGYPT**
2. Department of Chemistry, Faculty of Science, Suez Canal University, Ismailia, **EGYPT**

Email: asfouda@hotmail.com

Accepted on 21st January 2017, Published online on 27th January 2017

ABSTRACT

Asafoetida extract (ASF) was investigated as a green corrosion inhibitor for Cu in 1 M HNO_3 solution using weight loss (WL), potentiodynamic polarization (PP), electrochemical impedance spectroscopy (EIS) and electrochemical frequency modulation (EFM) techniques. Surface morphology was tested using scanning electron microscope (SEM). The effect of the temperature on corrosion behavior with addition of different doses was studied in the temperature range of 25-45 ºC by WL. Polarization curves reveal that the investigated extract is a cathodic behavior. The inhibition efficiency (IE) was found to increase with increase in the investigated extract dose and decrease with increase in solution temperature. The adsorption of the inhibitor on Cu surface was found to obey the Langmuir's adsorption isotherm. The activation and adsorption parameters were calculated and discussed. The results obtained from chemical and electrochemical techniques are in good agreement.

Keywords: Acidic inhibition, Cu, Asafoetida extract (ASF), Green inhibitor, SEM.

INTRODUCTION

Corrosion is a fundamental process playing an important role in economics and safety, particularly for metals. The use of inhibitors is one of the most practical methods for protection against corrosion, especially in acidic media [1]. Most well-known acid inhibitor are organic compounds containing nitrogen, sulfur and oxygen atoms. Among them, organic inhibitors have many advantages such as high inhibition efficiency and easy production [2-5].Organic heterocyclic compounds have been used for the corrosion inhibition of iron [6-9], Cu [10], aluminum [11-13] and other metals [14-15] in different corroding media. Although many of these compounds have high inhibition efficiencies, several have undesirable side effects, even in very small doses, due to their toxicity to humans, deleterious environmental effects and high-cost [16].

Plant extract is low-cost and environmental safe, so the main advantages of using plant extracts as corrosion inhibitor are economic and safe environment. Up till now, many plant extracts have been used as effective corrosion inhibitors for Cu in acidic media such as: Zenthoxylum alatum [17], Azadirachta Indica [18], caffeine [19] Cannabis [20], Capsicum extract [21]. The inhibition performance of plant extract is

normally ascribed to the presence of complex organic species, including tannins, alkaloids and nitrogen bases, carbohydrates and proteins as well as hydrolysis products in their composition. These organic compounds usually contain polar functions with nitrogen, sulfur, or oxygen atoms and have triple or conjugated double bonds with aromatic rings in their molecular structures, which are the major adsorption centers.

Asafoetida (ASF) is a small genus of flowering plants in the nightshade family, Apiaceae. The eleven species it contains are known generally as the henbanes, is widely distributed in Mediterranean, The whole plant has great medicinal importance, as a poultice to relieve pain, the main constituent of this extract is umbelliferone by growth stage and among populations may be reasons for variations in its toxicity and its value as fodder [18].

The present work was designed to study the inhibitory action of Asafoetida (ASF) for the corrosion of Cu in 1 M HNO_3 using WL, PP, EIS, EFM techniques, and Surface morphology was tested using scanning electron microscope (SEM).

MATERIALS AND METHODS

Materials and Solutions: Experiments were performed using Cu specimens (99.98%) were mounted in Teflon. An epoxy resin was used to fill the space between Teflon and Cu electrode. The auxiliary electrode was a platinum wire (1.2 cm^2), while a saturated calomel electrode (SCE) connected to a conventional electrolytic cell of capacity 100 mL via a bridge with a Luggin capillary, the tip of which was very close to the surface of the working electrode to minimize the IR drop. The aggressive solution used was prepared by dilution of analytical reagent grade 70% HNO_3 with bidistilled water. The stock solution (1000 ppm) of ASF was used to prepare the desired doses by dilution with bidistilled water. The dose range of ASF used was 50-300 ppm.

Preparation of plant extracts: Fresh aerial parts of ASF sample were crushed to make fine powder. The powdered materials (250 g) were soaked in 500 ml of dichloromethane for 5 days and then subjected to repeated extraction with 5× 50 mL until exhaustion of plant materials. The extracts obtained were then concentrated under reduced pressure using rotary evaporator at temperature below 50°C. The dichloromethane evaporated to give solid extract that was prepared for application as corrosion inhibitor. Chemical studies have demonstrated that the ASF contains many alkaloids as Hyoscine, Atropine and Hyoscyanine as the major compounds [22].

WL measurements: Seven parallel Cu sheets of 1×1×0.4 cm were abraded with emery paper (grade 320–500–1200) and then washed with bidistilled water and acetone. After accurate weighing, the specimens were immersed in a 250 mL beaker, which contained 100 mL of $HNO_3$with and without addition of different doses of ASF. All the aggressive acid solutions were open to air. After 180 minutes, the specimens were taken out, washed, dried, and weighed accurately. The average weight loss of seven parallel Cu sheets could be obtained. The inhibition efficiency (IE %) and the degree of surface coverage, θ of ASF for the corrosion of Cu were calculated as follows [23],

$$IE\% = \theta \times 100 = \left[1 - \frac{W}{W^{\circ}}\right] \times 100 \quad (1)$$

where W^o and W are the values of the average weight loss without and with addition of the inhibitor, respectively.

Electrochemical measurements: Electrochemical measurements were performed using a typical three-compartment glass cell consisting of the Cu specimen as working electrode (1 cm^2), saturated calomel electrode (SCE) as a reference electrode, and a platinum wire as a counter electrode. The reference electrode was connected to a Luggin capillary and the tip of the Luggin capillary is made very close to the surface of the working electrode to minimize IR drop. All the measurements were done in solutions open

to atmosphere under unstirred conditions. All potential values were reported versus SCE. Prior to each experiment, the electrode was abraded with successive different grades of emery paper, degreased with acetone, also washed with bidistilled water, and finally dried. Tafel polarization curves were obtained by changing the electrode potential automatically from (-0.8 to 1 V vs. SCE) at open circuit potential with a scan rate of 1 mVs^{-1}. Stern-Geary method [24], used for the determination of corrosion current is performed by extrapolation of anodic and cathodic Tafel lines to a point which gives (log i_{corr}) and the corresponding corrosion potential (E_{corr}) for inhibitor free acid and for each dose of inhibitor. Then (i_{corr}) was used for calculation of inhibition efficiency (IE %) and surface coverage (θ) as in equation 2:

$$IE\ \% = \Theta \times 100 = \left[1 - \frac{i_{corr\ (inh)}}{\mathrm{i}corr_{\ (free\ )}}\right] \times 100 \qquad (2)$$

where $i_{corr(free)}$ and $i_{corr(inh)}$ are the corrosion current densities in the nonexistence and existenceof inhibitor, respectively .

Impedance measurements were carried out in frequency range ($2x10^4$ Hz to $8x10^{-2}$ Hz) with amplitude of 10 mV peak-to-peak using ac signals at open circuit potential. The experimental impedance was analyzed and interpreted based on the equivalent circuit. The main parameters deduced from the analysis of Nyquist diagram are the charge transfer resistance R_{ct} (diameter of high-frequency loop) and the double layer capacity C_{dl}. The IE% and the surface coverage (θ) obtained from the EIS measurements are calculated from equation 3:

$$IE\% = \Theta \times 100 = \left[1 - \left(\frac{R^{\circ}_{ct}}{R_{ct}}\right)\right] \times 100 \qquad (3)$$

where R^{o}_{ct} and R_{ct} are the charge transfer resistance in the nonexistence and existence of inhibitor, respectively.

EFM was carried out using two frequencies 2 and 5 Hz. The base frequency was 0.1 Hz, so the waveform repeats after 1 s. The higher frequency must be at least two times the lower one. The higher frequency must also be sufficiently slow that the charging of the double layer does not contribute to the current response. Often, 10 Hz is a reasonable limit. The Intermodulation spectra contain current responses assigned for harmonically and intermodulation current peaks. The large peaks were used to calculate the corrosion current density (i_{corr}), the Tafel slopes (β_a and β_c) and the causality factors CF-2&CF-3[25]. The electrode potential was allowed to stabilize 35 min before starting the measurements. All the experiments were conducted at 25°C.

All electrochemical measurements were performed using Gamry Instrument (PCI4/750) Potentiostat/Galvanostat/ZRA. This includes a Gamry framework system based on the ESA 400. Gamry applications include DC105 software for potentiodynamic polarization, EIS300 software for electrochemical impedance spectroscopy, and EFM140 software for electrochemical frequency modulation measurements via computer for collecting data. Echem Analyst 6.03 software was used for plotting, graphing, and fitting data. To test the reliability and reproducibility of the measurements, duplicate experiments, this was performed in each case at the same conditions.

Surface morphology: For morphological study, surface features (1 cm x 1 cm x 0.4cm) of Cu were examined before and after exposure to one M HNO_3 solutions for one day with and without inhibitor. JEOL JSM-5500 scanning electron microscope was used for this investigation.

RESULTS AND DISCUSSION

WL measurements: WL measurements were carried out for Cu in 1 M HNO_3 in the nonexistence and existence of different doses of ASF and are shown in figure (1). The IE % values calculated are listed in tables 1, 2. From these Tables, it is noted that the IE% increases steadily with increasing the dose of ASF and decrease with temperature rising from 25-45ºC. The IE % and θ were calculated by equation (1).

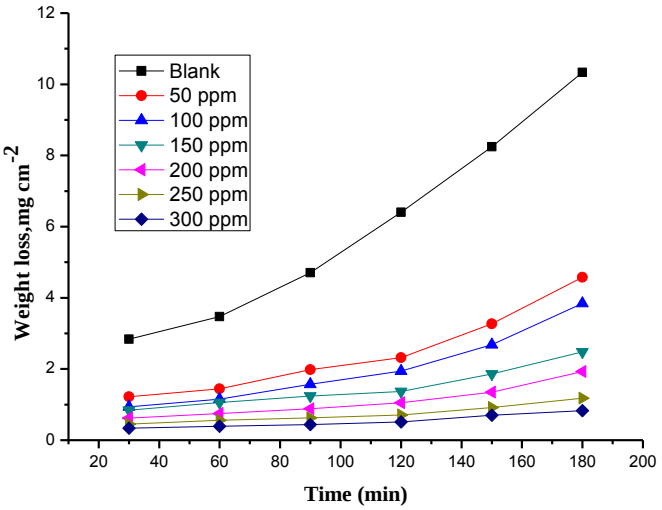

Figure 1. WL-time plots for the corrosion of Cu in 1 M HNO_3 in the nonexistence and existence of different doses of ASF at 25°C.

Table 1. Corrosion rate (C.R.) and IE data obtained from WL measurements for Cu in 1 M HNO_3 solutions without and with various doses of ASF at 25°C

Conc., ppm	C.R., mg cm^{-2} min^{-1}	θ	%IE
1 M HNO_3	0.012	---	---
50	0.009	0.646	64.6
100	0.007	0.724	72.4
150	0.004	0.795	79.5
200	0.003	0.873	87.3
250	0.001	0.913	91.3
300	0.012	0.959	95.9

Table 2. Data of WL measurements for Cu corrosion in 1 M HNO_3 solution in the nonexistence and existence of different doses of ASF at different temperatures

Conc., ppm	Temp., °C	C.R., (mg $cm^{-2}min^{-1}$)	θ	% IE
50	25	0.012	0.646	64.6
	30	0.019	0.638	63.8
	35	0.024	0.582	58.2
	40	0.035	0.490	49.0
	45	0.044	0.445	44.5
100	25	0.009	0.724	72.4
	30	0.016	0.697	69.7
	35	0.020	0.656	65.6
	40	0.028	0.586	58.6
	45	0.036	0.550	55.0
150	25	0.007	0.795	79.5
	30	0.011	0.786	78.6
	35	0.014	0.760	76.0
	40	0.022	0.685	68.5
	45	0.030	0.629	62.9
200	25	0.004	0.873	87.3
	30	0.009	0.836	83.6
	35	0.010	0.829	82.9
	40	0.014	0.801	80.1
	45	0.021	0.735	73.5

250	25	0.003	0.913	91.3
	30	0.006	0.889	88.9
	35	0.008	0.867	86.7
	40	0.011	0.837	83.7
	45	0.015	0.812	81.2
300	25	0.001	0.959	95.9
	30	0.004	0.920	92.0
	35	0.007	0.880	88.0
	40	0.008	0.877	87.7
	45	0.012	0.852	85.2

The observed inhibition action of the ASF could be attributed to the adsorption of its components on Cu surface. The formed layer, of the adsorbed molecules, isolates the metal surface from the aggressive medium which limits the dissolution of the latter by blocking of their corrosion sites and hence decreasing the corrosion rate, with increasing efficiency as their doses increase [26].

Polarization curves: Figure 2 shows potentiodynamic polarization curves recorded for Cu in 1 M HNO_3 solutions in the nonexistence and existence of various doses of ASF at 25ºC. Lee and Nobe [27] reported the occurrence of a current peak between the apparent-Tafel and limiting-current regions during potential sweep experiments. The presence of ASF shifts both anodic and cathodic branches to the lower values of corrosion current densities and thus causes a remarkable decrease in the corrosion rate. The parameters derived from the polarization curves in figure 2 are given in table 3. In 1 M HNO_3 solution, the presence of ASF causes a remarkable decrease in the corrosion rate i.e., shifts both anodic and cathodic curves to lower current densities. In other words, both cathodic and anodic reactions of Cu electrode are retarded by ASF in 1 M HNO_3 solution. The Tafel slopes of β_a and β_c at 25ºCdo not change remarkably upon addition of ASF, which indicates that the presence of ASF does not change the mechanism of hydrogen evolution and the metal dissolution process. Generally, an inhibitor can be classified as cathodic type if the shift of corrosion potential in the presence of the inhibitor is more than 85 mV with respect to that in the absence of the inhibitor [28, 29]. In the presence of ASF, E_{corr} shifts to less negative but this shift is very small (about 20-30 mV), which indicates that ASF can be arranged as cathodic inhibitor.

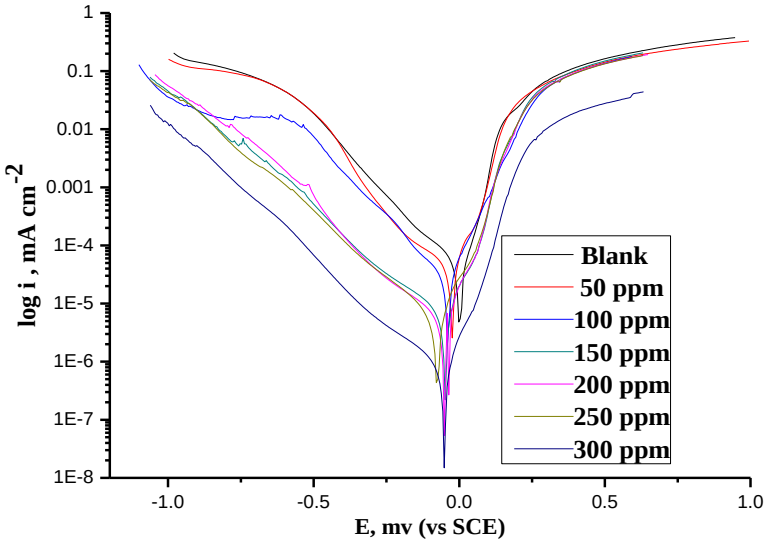

Figure 2. PP curves for the corrosion of Cu in 1 M HNO_3 solution without and with various doses of ASF at 25˚C

Table 3. Effect of doses of ASF on the electrochemical parameters calculated using PP technique for the corrosion of Cu in 1 M HNO_3 at 25˚C

Conc., ppm	i_{corr}, µA cm^{-2}	$-E_{corr}$, mV vs. SCE	β_a, $mVdec^{-1}$	β_c, $mVdec^{-1}$	CR, mm y^{-1}	θ	IE %
1 M HNO_3	125	11.7	94	219	190	--	--
50	48	10.1	86	206	68	0.616	61.6
100	32	10.9	89	190	55	0.744	74.4
150	28	13.1	78	201	38	0.776	77.6
200	21	15.4	75	189	29	0.832	83.2
250	18	18.2	68	193	24	0.856	85.6
300	10	18.5	65	197	15	0.92	92.00

EIS tests: Figure 3 shows impedance plots for Cu in 1 M HNO_3 solution without and with different doses of ASF extract. The impedance spectra consists of a Nyquist semicircle type without appearance of diffusive contribution to the total impedance (Z) indicating that the corrosion proceeds mainly under charge-transfer control and the presence of inhibitor do not alter the mechanism of corrosion reaction. It is found that the obtained Nyquist plots are not perfect semicircle due to frequency dispersion and this behavior can be attributed to roughness and in homogeneities of the electrode surface [30, 31]. When there is non-ideal frequency response, it is common practice to use distributed circuit elements in an equivalent circuit. The most widely employed is the constant phase element (CPE). In general a CPE is used in a model in place of a capacitor to compensate for in homogeneity in the system [32]. It was found that the diameters of the semicircle increases with increasing the dose of the investigated extract. This indicates that the polarization resistance of the oxide layer increases with increasing the dose of ASF and the depressed capacitive semicircle are often referred to the surface roughness and in homogeneity, since this capacitive semicircle is correlated with dielectric properties and thickness of the barrier oxide film [33]. The data revealed that, each impedance diagram consists of a large capacitive loop with low frequencies dispersion (inductive arc). This inductive arc is generally attributed to anodic adsorbed intermediates controlling the anodic process [34-36]. By following this, inductive arc was disregarded.

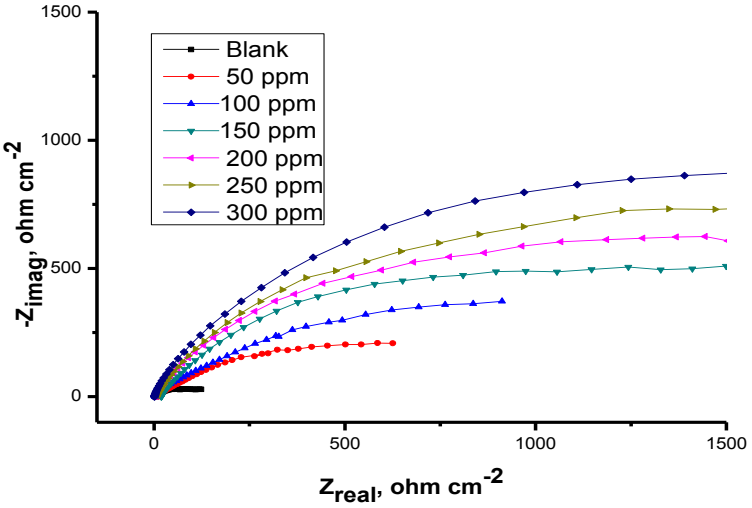

Figure 3. Nyquist plots for Cu in 1 M HNO_3 solutions in the nonexistence and existence of various doses of ASF at 25°C

The electrical equivalent circuit model shown in figure 4 was used to analyze the obtained impedance data. The model consists of the solution resistance (R_s), the charge-transfer resistance of the interfacial corrosion reaction (R_{ct}) and the constant phase angle element (CPE with diffusion). The value of frequency power

(n) of CPE can be assumed to correspond to capacitive behavior. However, excellent fit with this model was obtained with our experimental data. The admittance of CPE is described as:

$$Y_{CPE} = Y_o(j\omega)^n \quad (4)$$

where j is the imaginary root, ω the angular frequency, Y_o the magnitude and *n* the exponential term [37].

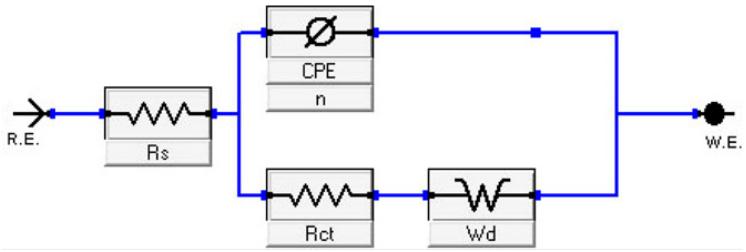

Figure 4: Equivalent circuit used to model impedance data for Cu in 1 M HNO_3 solutions

A long Warburg diffusion tail was observed at low frequency values. The tails are inclined at an angle of 45° to the real-axis at the very low frequencies; A diffusion controlled process is therefore exists. Studies reported in the literature [38] showed that the diffusion process is controlled by diffusion of dissolved oxygen from the bulk solution to the electrode surface and the Warburg impedance, which is observed in the low frequency regions, is ascribed to diffusion of oxygen to the alloy surface. This diffusion tail still appears, even in presence of high doses of the investigated extract. This means that the corrosion behavior of alloy in the absence as well as in the presence of ASF is influenced by mass transport. Also, Bode plots for the Cu in 1 M HNO_3 solution are shown in figure 5. In which the high frequency limit corresponding to the electrolyte resistance (ohmic resistance) R_Ω, while the low frequency represents the sum of (R_Ω + R_{ct}), where R_{ct} is in the first approximation determined by both electrolytic conductance of the oxide film and the polarization resistance of the dissolution and repassivation process. At both low and high frequency limits, the phase angle between the current and potential (θ), assumes a value of about 0°, corresponding to the resistive behavior of R_Ω and (R_Ω + R_{ct}).

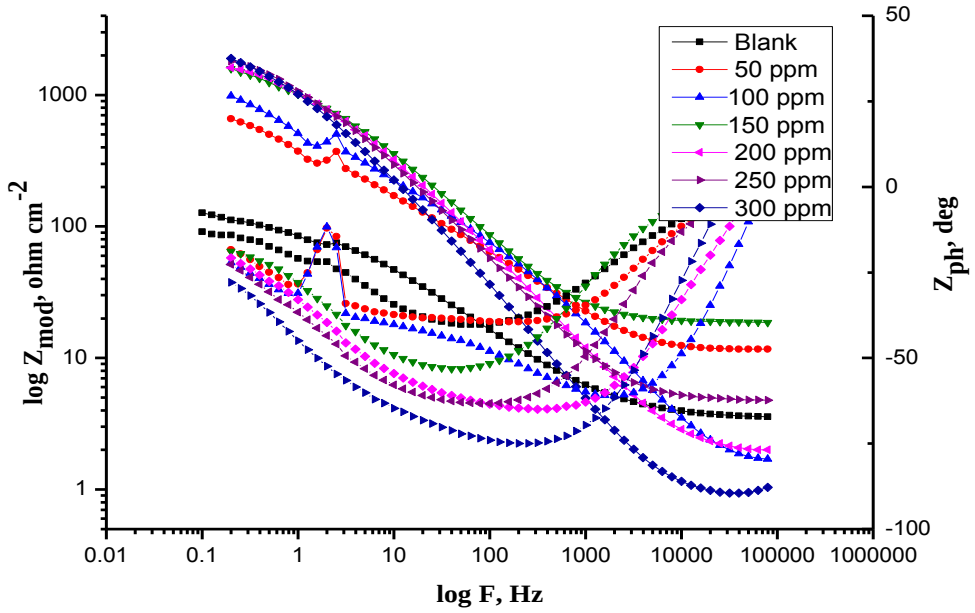

Figure 5: Bode plots for Cu in 1M HNO_3 solutions in the nonexistence and existence of various ASF doses at 25°C

The main parameters deduced from the analysis of Nyquist diagram are: The resistance of charge transfer R_{ct} (diameter of high frequency loop). The capacity of double layer C_{dl} which is defined as:

$$C_{dl} = \frac{1}{2\pi R_{ct} f_{max}} \quad (5)$$

where f_{max} is the maximum frequency at which the Z_{imag} of the impedance is a maximum. Since the electrochemical theory assumed that $(1/R_{ct})$ is directly proportional to the capacity of double layer C_{dl}, the inhibition efficiency (% IE) of the inhibitor for Cu in 1 M HNO_3 solution was calculated from R_{ct} values obtained from impedance data at different inhibitor dose the following equation:

$$\% IE = \left(1 - \frac{R^{\circ}_{ct}}{R_{ct}}\right) \times 100 \quad (6)$$

where R^{o}_{ct} and R_{ct} are the charge transfer resistance in the nonexistence and existence of investigated extract, respectively.

From the impedance data given in table 4, we can conclude that the value of R_{ct} increases with the increase in the dose of the investigated extract and this indicates the formation of a protective film on the alloy surface by the adsorption and an increase in the corrosion inhibition efficiency in acidic solution. While the value of C_{dl} decreases with increasing the doses of extract in comparison with that of blank solution (uninhibited), as a result from the replacement of water molecules by inhibitor molecules which lead to decrease in local dielectric constant and/or an increase in the thickness of the electric double layer formed on the metal surface [39,40].

Table 4: Parameters obtained for Cu in 1 M HNO_3 solutions in the nonexistence and existence of various doses of ASF at 25°C

Conc., ppm	R_{s_2} Ωcm	$Y^{0}_{x10^{-6}}$ $\Omega^{-1}s^{n}cm^{-2}$	n	R_{p_2} Ω cm	C_{dl}, x10^4 µF cm^{-2}	θ	%η
Blank	3.32	1547	0.588	124	220	---	---
50	1.13	506	0.553	710	190	0.825	82.5
100	1.14	198	0.669	746	120	0.834	83.4
150	1.71	140	0.706	1532	100	0.919	91.9
200	1.77	123	0.757	1671	91	0.926	92.6
250	4.4	140	0.761	1890	76	0.934	93.4
300	5.7	132	0.847	1985	70	0.938	93.8

EFM tests: EFM is a nondestructive corrosion measurement technique that can directly determine the corrosion current value without prior knowledge of Tafel slopes, and with only a small polarizing signal. These advantages of EFM technique make it an ideal candidate for online corrosion monitoring [41].

The great strength of the EFM is the causality factors which serve as an internal check on the validity of EFM measurement. The causality factors CF-2 and CF-3 are calculated from the frequency spectrum of the current responses. The EFM intermodulation spectrums of Cu in 1 M HNO_3 solution containing 300 ppm of the ASF extract at 25°C are shown in figure 6. The experimental EFM data were treated using two different models: complete diffusion control of the cathodic reaction and the "activation" model. For the latter, a set of three non-linear equations had been solved, assuming that the corrosion potential does not change due to the polarization of the working electrode [42].The larger peaks were used to calculate the corrosion current density (i_{corr}), the Tafel slopes (β_c and β_a) and the causality factors (CF-2 and CF-3).These electrochemical parameters were listed in table 5 indicating that this extract inhibits the corrosion of Cu in 1 M HNO_3 via adsorption. The causality factors obtained under different experimental conditions are approximately equal to the theoretical values 2 and 3 indicating that the measured data are verified and

of good quality [43]. The IE_{EFM} % increase by increasing the studied extract doses and was calculated as follows:

$$IE\ \%_{EFM} = \left(1 - \frac{i_{corr}}{i^{\circ}_{corr}}\right) \times 100 \quad (7)$$

where i^{o}_{corr} and i_{corr} are corrosion current densities in the nonexistence and existence of ASF extract, respectively.

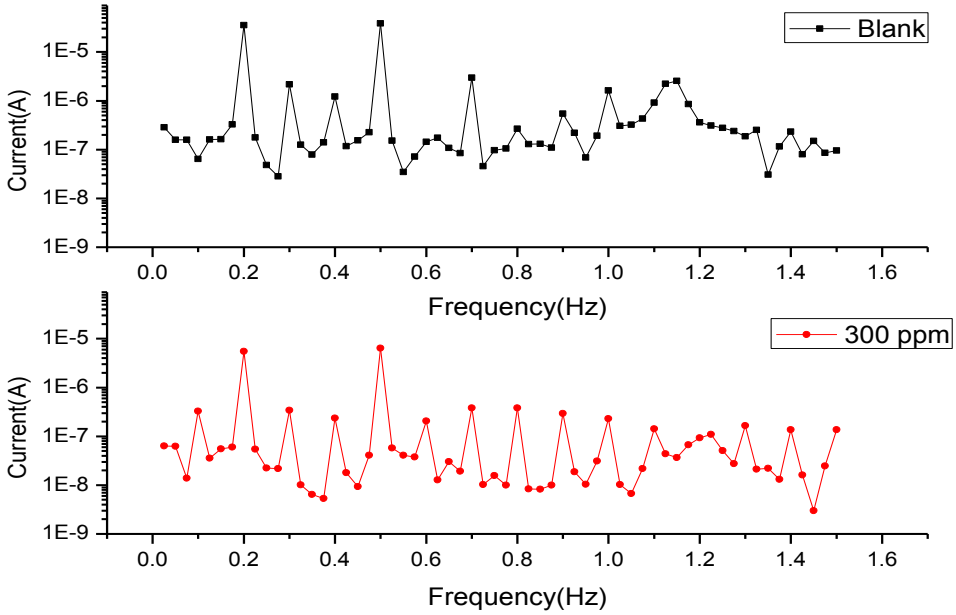

Figure 6: Intermodulation spectrums for the corrosion of Cu in 1 M HNO_3 without and with various doses of ASF at 25˚C

Table 5: Electrochemical kinetic parameters obtained by EFM technique for Cu in1 M HNO_3 solutions containing various doses of ASF at 25°C

Conc., ppm	i_{corr}, µA cm^{-2}	β_a mV dec^{-1}	β_c mV dec^{-1}	C.R. mpy	CF-2	CF-3	θ	% IE
1 M HNO_3	80.1	41	53	40	1.8	2.7	---	---
50	16.2	66	55	8.1	1.9	3.1	0.797	79.7
100	12.9	65	58	6.4	1.9	3.2	0.838	83.8
150	10.9	34	94	5.3	1.9	3.1	0.864	86.4
200	9.2	47	79	4.4	1.9	3.0	0.885	88.5
250	6.5	49	65	3.2	1.9	3.1	0.919	91.9
300	4.9	50	77	1.4	1.8	2.8	0.939	93.9

Adsorption isotherms: The mode and interaction degree between an inhibitor and a metallic surface have been widely studied with the application of adsorption isotherms. The adsorption of an organic molecule occurs because the interaction energy between an inhibitor and a metallic surface is higher than that between water molecules and metallic surface [44, 45]. To obtain the adsorption isotherms, the θ obtained from WL method was determined as a function of inhibitor dose. The values of θ were then plotted to fit the most suitable model of adsorption [46]. Attempts were made to fit experimental data to various isotherms including Frumkin, Langmuir, Temkin, Freundlich isotherms. By far the results were best fitted by Langmuir adsorption isotherm as seen in figure 7 [47]:

$$\frac{C}{\theta} = \frac{1}{K} + C \quad (8)$$

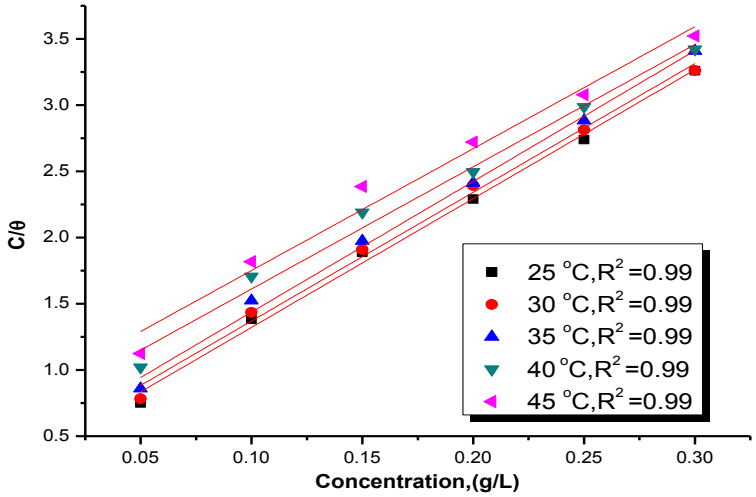

Figure7. Langmuir adsorption plots for Cu in 1 M HNO_3 containing various doses of ASF at 25°C

Table 6. Kinetic parameters for the corrosion of Cu in 1M HNO_3 at different temperatures

Temp, °C	K_{ads}, M^{-1}	$-\Delta G^{o}_{ads}$, kJ mol^{-1}	$-\Delta H^{o}_{ads}$, kJ mol^{-1}	ΔS^{o}_{ads}, J mol^{-1} K^{-1}
25	287	12.6	35	42.1
30	251	12.4		40.9
35	222	12.3		39.9
40	145	11.4		36.4
45	120	11.1		34.8

Kinetic-thermodynamic corrosion parameters: WL method was carried out at different temperatures (25°C–45°C) in the presence of different dose of ASF. It has been found that he corrosion rate increases with the increase in temperature for ASF table 2. The corrosion rate of Cu in the absence of ASF increased steeply from 25 to 45°Cwhereas; in the presence of ASF the corrosion rate decreased slowly. The inhibition efficiency was found to decrease with temperature. The corrosion parameter in the nonexistence and existence of extract in the temperature range 25–45°C has been summarized in table 2.The apparent activation energy (E^{*}_{a}) for dissolution of Cu in 1M HNO_3 was calculated from the slope of plots by using Arrhenius equation:

$$\log k = \frac{-E_a^*}{2.303\ R\ T} + \log A \qquad (9)$$

where k is rate of corrosion, E^{*}_{a} is the apparent activation energy is the universal gas constant, T is absolute temperature and A is the Arrhenius pre-exponential factor.

By plotting log k against 1/T the values of activation energy (E^{*}_{a}) has been calculated (E^{*}_{a} = (slope) 2.303 x R) Figure 8. Activation energy for the Cu in 1M HNO_3 increases with presence of extract table 6. This increase in activation energy E^{*}_{a} indicates the formation of chemical bonds were strengthen by increasing the temperature. However, the extent of the rate increment in the inhibited solution is higher than that in the free acid solution. Therefore, the inhibition efficiency of the ASF decreases markedly with increasing temperature. This result supports the idea that the adsorption of extract components on the Cu surface may be chemical in nature. Thus, as the temperature increases the number of adsorbed molecules increases leading to an increase in the IE. The obtained results suggest that ASF inhibits the corrosion reaction by improving its activation energy. This could be done by adsorption on the Cu surface making a barrier for mass and charge transfer. However, such types of inhibitors perform a good inhibition at high temperature

with considerable increase in IE at elevated temperatures [48]. Moreover, the relatively low value of activation energy in presence of ASF suggests a physical adsorption process.

The values of change of entropy (ΔS^*) and change of enthalpy (ΔH^*) can be calculated by using the formula:

$$k = \left(\frac{RT}{Nh}\right) exp\left(\frac{\Delta S^*}{R}\right) exp\left(\frac{\Delta H^*}{RT}\right) \quad (10)$$

where k is rate of corrosion, h is Planck's constant, N is Avogadro number, ΔS^* is the entropy of activation and ΔH^* is the enthalpy of activation. A plot of log (k/T) vs. 1/T figure 9 should give a straight line, with a slope of (ΔH^*/2.303R) and an intercept of [log (R/Nh)+ΔS^*/2.303R], from which the values of ΔS^* and ΔH^* can be calculated table 7.The negative value of ΔS^* for the inhibitor indicates that activated complex in the rate determining step represents an association rather than a dissociation step, meaning that a decrease in disorder takes place during the course of transition from reactant to the activated complex [49] The negative sign of ΔH^* indicates that the adsorption of extract molecules is an exothermic process. Generally exothermic process signifies physisorption, chemisorptions or a combination of both.

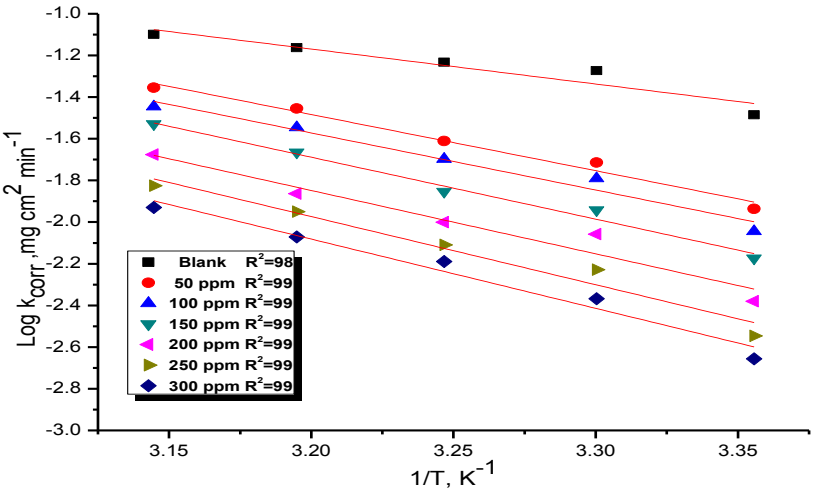

Figure 8. Log k (corrosion rate) – 1/T curves for Cu in 1 M HNO_3 in the nonexistence and existence of different doses of ASF.

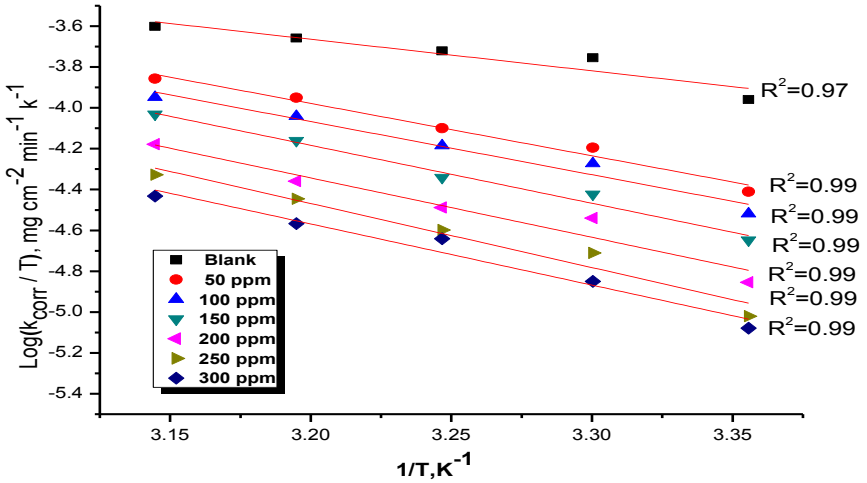

Figure 9. Log k (corrosion rate) /T – 1/T curves for Cu in 1 M HNO_3in the nonexistence and existence of different doses of ASF.

Table 7. Activation parameters for dissolution of Cu in the nonexistence and existence of different doses of ASF in 1 M HNO_3

Conc, ppm	E_a^*, kJ mol^{-1}	ΔH^*, kJ mol^{-1}	$-\Delta S^*$, J $mol^{-1}K^{-1}$
1.0 M HNO_3	32.1	29.6	172.9
50	51.7	48.9	116.5
100	52.4	49.8	115.8
150	56.9	54.3	103.7
200	58.2	55.7	102.5
250	62.6	60.1	90.81
300	79.8	77.3	37.7

Surface analysis by SEM: Figure 10 shows an SEM photograph recorded for Cu samples Polished (A) and exposed for one day in 1M HNO_3 solution without (B) and with 300 ppm of ASF at $25C^0$. A photograph of the polished Cu surface before immersion in 1 M HNO_3 solution is shown in figure 10a. The photograph shows the surface was smooth and without pits. The SEM micrographs of the corroded Cu in the presence of 1 M HNO_3 solution are shown in figure 10b. The faceting seen in this figures was a result of pits formed due to the exposure of Cu to the acid. The influence of the inhibitor addition 300 ppm on the Cu in 1 M HNO_3 solution is shown in figure 10c. The morphology in figure 10c shows a rough surface, characteristic of uniform corrosion of Cu in acid, as previously reported [50], that corrosion does not occur in presence of inhibitor and hence corrosion was inhibited strongly when the inhibitor was present in the nitric acid, and the surface layer is very rough. In contrast, in the presence of 300 ppm of ASF, there is much less damage on the Cu surface, which further confirm the inhibition action. Also, there is an adsorbed film adsorbed on Cu surface figure 10c. In accordance, it might be concluded that the adsorption film can efficiently inhibits the corrosion of Cu.

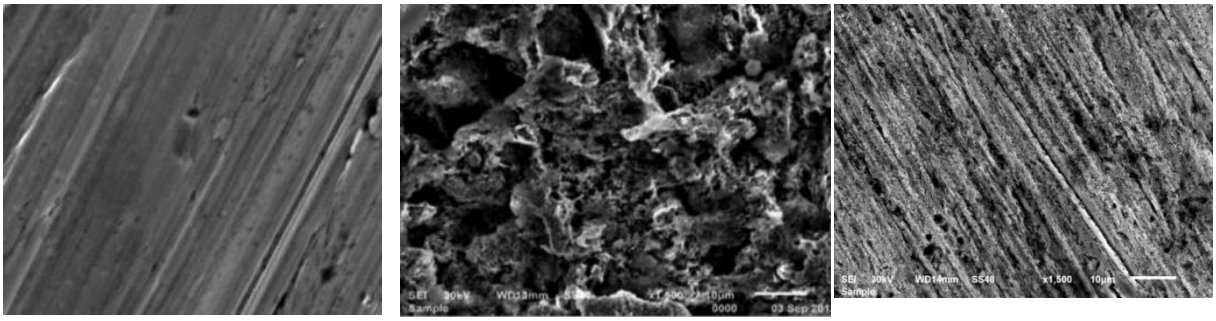

(a) **(b)** **(C)**

Figure 10: SEM micrographs of Cu surface (a) before of immersion in 1 M HNO_3, (b) after one day of immersion in 1 M $HNO_3$and (c) after 12 h of immersion in 1 M HNO_3 + 300 ppm of ASF at 25°C.

Mechanism of the corrosion inhibition: The adsorption of organic compounds can be described by two main types of interactions: physical adsorption and chemisorption. In general, physical adsorption requires the presence of both the electrically charged surface of the metal and charged species in solution. The surface charge of the metal is due to the electric field existing at the metal/solution interface. A chemisorption process, on the other hand, involves charge sharing or charge transfer from the inhibitor molecules to the metal surface to form a coordinate type of a bond. This is possible in case of a positive as well as a negative charge of the surface. The presence of a transition metal, having vacant, low-energy electron orbitals (Cu^+ and Cu^{2+}) and an inhibitor with molecules having relatively loosely bound electrons

or heteroatoms with a lone pair of electrons is necessary for the inhibiting action [51]. Generally, two types of mechanisms of inhibition were proposed. One was the formation of polymeric complexes with Cu ions (Cu^{+} and Cu^{+2}) depending on the applied conditions [52, 53]. The other was the chemical adsorption of ASF on Cu surfaces [54, 55]. The inhibition action of ASF does not occur by the simple blocking at the surface of Cu, especially at high temperature. This might be attributed to the different adsorption capacities of the ASF extract on the Cu surface at different temperatures. It has been studied that with the increase in temperature, the desorption effect of ASF on Cu surface decreased.

CONCLUSIONS

From the overall experimental results the following conclusions can be deduced:
1. The ASF shows good performance as corrosion inhibitor in 1 M HNO_3. 2. The results obtained from WL showed that the inhibiting action increases with the increase in the ASF dose and decreases with the increasing the temperature. 3. Double layer capacitances decrease with respect to blank solution when the plant extract is added. This fact confirms the adsorption of plant extract molecules on the Cu surface.
4. The ASF inhibits the corrosion by getting adsorbed on the metal surface following Langmuir adsorption isotherm. 5. The IE% determined by WL, PP, EFM and EIS techniques are in reasonably good agreement.

REFERENCES

[1] G. Trabanelli, C. Montecelli, V. Grassi, A. Frignani, *J. Cem. Concr. Res.*, **2005**, 35, 1804-1813.
[2] D. N. Singh, A. K. Dey, *Corrosion*, **1993**, 49, 594-600.
[3] G. Banerjee, S. N. Malhotra, *Corrosion*, **1992**, 48, 10-15.
[4] S. T.Arab, E. A.Noor, *Corrosion*, **1993**, 49, 122-129.
[5] I. A.Raspini, *Corrosion*, **1993**, 49, 821-828.
[6] A. Khadraoui, A. Khelifa, L. Touafri, H. Hamitouche, R. Mehdaoui, *J. Mater. Environ. Sci*, **2013**, 4, 663-670
[7] M. Elachouri, M. S.Hajji, M. Salem, S. Kertit, R. Coudert, E. M. Essassi, *Corros.Sci.*, **1995**, 37, 381-398.
[8] H. Luo, Y. C. Guan, K. N. Han, *Corrosion*, **1998**, 54, 619-627.
[9] M. A. Migahed, E. M. S. Azzam, A. M. Al-Sabagh, *Mater. Chem.Phys*, **2004**, 85, 273-279.
[10] R. F. V.Villamil, P.Corio, J. C.Rubim, M. L.Siliva Agostinho, *J. Electroanal. Chem*, **1999**, 472, 112-118.
[11] H. Kumar, S.Karthikeyan, *J. Mater. Environ. Sci.*, **2012**, 3 (5), 925–934.
[12] M. Pushpanjali, A. Suma, R. Padmalatha, *J. Mater. Environ. Sci.*, **2014**, 5 (2), 591-598
[13] S. S. Abd El Rehim, H. Hassan, M. A. Amin, *Mater.Chem.Phys.*, **2003**, 78, 337-348
[14] R. Guo, T. Liu, X. Wei, *Colloids Surf*, **2002**, A, 209, 37-45.
[15] V. Branzoi, F. Golgovici, F. Branzoi, *Mater.Chem.Phys*, **2002**, 78, 122-131.
[16] K. S. Parikh, K. J.Joshi, *Trans. SAEST*, **2004**, 39, 29-35.
[17] J. S. Chauhan, *Asian Journal of Chemistry*, **2009**, 21, 1975-1978.
[18] T. V. Sangeetha, M. Fredimoses, *E-Journal of Chemistry*, **2011**, 8(S1), S1-S6.
[19] Fernando Sílvio de Souza, Cristiano Giacomelli, Reinaldo Simões Gonçalves, Almir Spinelli, *Mater.Sci.Eng.*, **2012**, 32, 2436-2444.
[20] B. A. Abd-El-Nabey, A. M. Abdel-Gaber, M. El. Said Ali, E. Khamis, S. El-Housseiny, *J. Electrochem. Sci.*, **2013**, 8, 5851-5865.
[21] A. S. Fouda, M.El- Morsi, H. A. Mosallam**,** Zastita Materijala, **2016**, 57(1), 33-45
[22] G. N. Mu, T. P. Zhao, M. Liu, T. Gu, *Corrosion*, **1996**, 52, 853-856.
[23] R. G. Parr, R. A. Donnelly, M. Levy, W. E. Palke, *J. Chem. Phys.*, **1978**, 68, 3801-3807.
[24] R. W. Bosch, J. Hubrecht, W. F. Bogaerts, B. C. Syrett, *Corrosion*, **2001**, 57, 60-70.
[25] D. Q. Zhang, Q. R. Cai, X. M. He, L. X. Gao, G. S.Kim, *Mater. Chem. Phys.*, **2009**, 114, 612-617.
[26] H. P. Lee, K. Nobe, *J. Electrochem. Soc.*, **1986**, 133, 2035- 2043.

[27] Z. H. Tao, S. T. Zhang, W. H. Li, B. R. Hou, *Corros. Sci.*, **2009**, 51, 2588-2595.
[28] E. S. Ferreira, C. Giacomelli, F. C. Giacomelli, A. Spinelli, *Mater. Chem.Phys*, **2004**, 83, 129-134.
[29] L. Mounim, T.Michel, L.Michel, M.Bouchaib, *Corros. Sci*., **2008**, 50(2), 473–479
[30] F. B. Growcock, J. H. Jasinski, *J. Electrochem. Soc.*, **1989**, 136, 2310-2323.
[31] S. S. Abdel–Rehim, K. F. Khaled, N. S. Abd–Elshafi, *Electrochim. Acta* , **2006**, 51, 3269-3277.
[32] M. Metikos, R. Hukovic, Z. Bobic S.Gwabac, *J. Appl. Elactrochem.*, **1994**, 24, 772-778.
[33] A. Caprani, I. Epelboin, Ph. Morel, H. Takenouti, proceedings of the 4th European sym. On Corros. Inhibitors, **1975**, 571.
[34] J. Bessone, C. Mayer, K. Tuttner, W.Lorenz, *Electrochim. Acta*, **1983**, 28, 171-175
[35] I. Epelboin, M. Keddam, H.Takenouti, *J. Appl. Electrochem.*, **1972**, 2, 71-79.
[36] A. V. Benedeti, P. T. A. Sumodjo, K. Nobe, P. L. Cabot, W. G. Proud, *Electrochim. Acta*, **1995**, 40, 2657-2668.
[37] H. Ma, S. Chen, L. Niu, S. Zhao, S.Li, D.Li, *J. Appl. Electrochem.*, **2002**, 32, 65.72.
[38] X. H.Li, S. D. Deng, H. Fu, *J. Appl. Electrochem.*, **2010**, 40, 1641-1649.
[39] M. Lagrenee, B. Mernari, M. Bouanis, M. Traisnel, F. Bentiss, *Corros. Sci.*, **2002**, 44, 573-588.
[40] E. Kus, F. Mansfeld, *Corros. Sci.*, **2006**, 48, 965-979.
[41] G. A. Caigman, S. K. Metcalf, E. M. Holt, *J.Chem. Cryst.*, **2000**, 30, 415-422.
[42] R. R. Anand, R. M. Hurd, N. Hackerman, *J. Electrochem. Soc.* **1965**, 112, 138-144.
[43] J. O. Bockris, D. A. J. Swinkels, *J. Electrochem. Soc.*, **1964**, 111, 736-743.
[44] M. M. Saleh, A. A. Atia, *J. Appl. Electrochem*, **2006**, 36, 899-905.
[45] L. Narvez, E. Cano, D. M. Bastidas, *J. Appl. Electrochem.*, **2005**, 35, 499-506.
[46] X. H. Li, S. D. Deng, H. Fu, *Corros. Sci.*, **2009**, 51, 1344-1355.
[47] A. Popova, E.Sokolova, S. Raicheva, M.Christov, *Corros.Sci.*, **2003**, 45, 33-58
[48] V. R. Saliyan, A. V. Adhikari, *Bull. Mater*, **2008**, 31, 683-699.
[49] Y. Li, P. Zhao, Q. Liang, B.Hou, *Appl. Surf. Sci.*, **2005**, 252, 1245-1253.
[50] V. Saliyan, A. V. Adhikari, *Bull Mater Sci*, **2008**, 31, 699-711.
[51] V. Brusic, M. A. Frisch, B. N. Eldridge, F. P. Novak, G. S. Frankel, *J. Electrochem. Soc.*, **1991**, 138, 2253-2259.
[52] M. M. Antonijevic, M. B. Petrovic, *Int. J. Electrochem. Sci.*, 2008, 3, 1-28.
[53] M.M. Laz, R.M. Souto, S. González, *J Appl Electrochem*, **1992**, 22, 1129-1134.
[54] G. Lewis, *Corrosion*, **1978**, 34, 424-428.

AUTHOR ADDRESS

1. **A. S. Fouda**
Department of Chemistry,
Faculty of Science,
Mansoura University,
Mansoura-35516, Egypt
E-mail:asfouda@hotmail.com,
Tel: +2 050 2365730, Fax: +2 050 2365730